Supplementary Information for Shortcuts to equilibrium with a levitated particle in the underdamped regime

Damien Raynal,[1] Timothée de Guillebon,[1] David Guéry-Odelin,[2]
Emmanuel Trizac,[3] Jean-Sébastien Lauret,[1] and Loïc Rondin[1, *]

[1]*Université Paris-Saclay, ENS Paris-Saclay, CNRS,*
CentraleSupélec, LuMIn, 91405 Orsay Cedex, France
[2]*Université Paul Sabatier - Toulouse 3, CNRS,*
LCAR, 31062 Toulouse Cedex 9, France
[3]*Université Paris-Saclay, CNRS, LPTMS, 91405 Orsay Cedex, France*

(Dated: June 16, 2023)

I. EXPERIMENTAL METHODS

The particle is optically trapped at the focus of a NA=0.85 objective (Olympus LCPLN100XIR) using a high-power near-infrared laser beam (Coherent Mephisto MOPA up to 7 W, $\lambda = 1064$ nm). The laser power is tuned using an acousto-optics Modulator (AA Opto-Electronic MT110-A1.5-IR) driven with a fast arbitrary wave generator (Spectrum Instrumentation M4i.6621-x8). The particle dynamics are measured with a common path interferometer using an ancillary laser beam (Laser Quantum GEM, $\lambda_{\mathrm{meas}} = 532$ nm, $P_{\mathrm{meas}} \approx 7$ mW) and a quadrant photodetector (Hamamatsu S4349). The 3D dynamics of the particle is recorded onto a digital scope (Picoscope 4824A) at 5 MSamples/s. The particle position $x(t)$ is corrected by subtracting its mean value at equilibrium after each protocol realization, to eliminate experimental drifts.

II. DAMPING Γ OF LEVITATED PARTICLES

For a spherical particle of radius r in a rarefied gas, the damping rate Γ is directly proportional to the gas pressure p_{gas} [1]:

$$\Gamma = 0.619 \frac{9}{\sqrt{2\pi}\rho_{\mathrm{SiO_2}}} \sqrt{\frac{M}{N_A k_B T}} \frac{p_{\mathrm{gas}}}{r} \, , \tag{S1}$$

where $\rho_{\mathrm{SiO_2}} \approx 2200$ kg/m^3 is the silica density, M the molar mass of air, T the environment temperature.
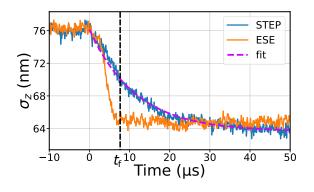
Considering the silica particle used in the main text, of expected radius $r = 73$ nm as given by the provider (microParticles GmbH), we find a damping rate $\Gamma_{\mathrm{theo}} = 2\pi \times 3.8$ kHz at a pressure $p_{\mathrm{gas}} = 5$ hPa.

Experimentally, this damping can be measured for pressures above a few hPa directly from the linewidth of the particle dynamics power spectral density [1], or alternatively, as discussed in the main text, from the relaxation time in a STEP protocol.

Using the second approach, we find $\Gamma_{\mathrm{exp}} = 2\pi \times 3.1$ kHz. This result is in good agreement with the expected value Γ_{theo}.

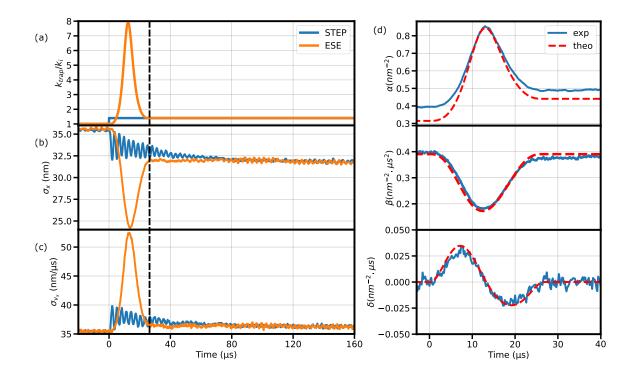* loic.rondin@universite-paris-saclay.fr

III. OVERDAMPED ESE PROTOCOLS

Supplementary Figure S1. Overdamped STEP (blue) and ESE (orange) compression protocols for the z-axis of an optically trapped particle in air. The purple dashed line correspond to an exponential fit, giving a relaxation time $t_z = 11.5$ µs.

As mentioned in the main text, and detailed in the Supplementary Note S1, our experimental apparatus allows to easily change the damping condition by tuning the gas pressure inside the vacuum chamber. This allows to address ESE protocols for a broad range of damping conditions. Specifically, it is possible to study overdamped protocols [2]. As a proof of principle, figure S1 shows the case of an overdamped compression with $\chi = 1.4$ for the z-axis, realized at ambient pressure $p_{\mathrm{gas}} = 10^5$ hPa ($\Gamma = 2\pi \times 570$ kHz $\gg \omega_z^f = 2\pi \times 92$ kHz). The reference STEP protocol (in blue) shows the expected position relaxation time toward equilibrium $t_z = \frac{\Gamma}{(\omega_z^f)^2}$. The ESE protocols (orange) allows us to shortcut the equilibration time by a factor 4, to $t_f = 8$ µs.

IV. ESE PROTOCOLS FOR COMPRESSION

Supplementary Figure S2. (a) Evolution of the trap stiffness for a harmonic compression in the case of a STEP protocol (blue line) and an ESE protocol corresponding to $\chi = 1.4$ and $t_f = 26$ µs (5-fold speed-up)(orange). (b) and (c) Evolution of the standard deviation in position σ_x (b) and velocity σ_{v_x} (c) for the STEP (blue) and the ESE protocol (orange) presented in (a). The black dotted vertical line corresponds to the final time $t_f = 26$ µs of the ESE protocol. (d) Evolution of α, β and δ (as defined in text) during the out-of-equilibrium regime of the ESE protocol pictured in (a). The experimental values (blue) are compared with those calculated for the ESE protocol (dashed red line).

V.   EVOLUTION OF VARIANCE FOR STEP PROTOCOLS

Let's consider a 1D harmonic potential, along the x axis, defined by its angular frequency $\omega(t)$. A particle of mass m is trapped in the harmonic potential at a temperature T_0, and the system damping is Γ. We introduce

$$
\begin{cases}
\sigma_{xx} = & \langle x^2 \rangle - \langle x \rangle^2 \\
\sigma_{xv} = & \langle xv \rangle - \langle x \rangle \langle v \rangle \\
\sigma_{vv} = & \langle v^2 \rangle - \langle v \rangle^2
\end{cases}
$$

These quantities are coupled through the linear system [3]:

$$
\frac{\mathrm{d}}{\mathrm{d}t}
\begin{pmatrix} \sigma_{xx} \\ \sigma_{xv} \\ \sigma_{vv} \end{pmatrix}
=
\begin{pmatrix}
0 & 2 & 0 \\
-\omega^2 & -\Gamma & 1 \\
0 & -2\omega^2 & -2\Gamma
\end{pmatrix}
\begin{pmatrix} \sigma_{xx} \\ \sigma_{xv} \\ \sigma_{vv} \end{pmatrix}
+
\begin{pmatrix} 0 \\ 0 \\ \dfrac{2k_B T_0 \Gamma}{m} \end{pmatrix}
\tag{S2}
$$

We address a STEP protocol, where the trap frequency is suddenly changed from ω_i to $\omega_f = \sqrt{\chi}\omega_i$ at $t = 0$. Following the main text notation, χ is the expansion factor. Solving this set of equations for the initial conditions $\sigma_{xx}(0) = \sigma_i$ and $\sigma_{vv}(0) = \sigma_i \omega_i^2$ leads to
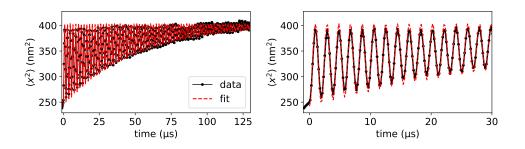
$$
\sigma_{xx}(t) = \sigma_i \frac{\chi - 1}{\chi} \left[\frac{2\omega_f^2}{\tilde{\Omega}^2} + \frac{2\omega_f^2 - \Gamma^2}{\tilde{\Omega}^2} \cos \tilde{\Omega}(t - t_0) + \frac{\Gamma}{\tilde{\Omega}} \sin \tilde{\Omega}(t - t_0) \right] e^{-\Gamma(t - t_0)} + \frac{\sigma_i}{\chi}, \tag{S3}
$$

with $\tilde{\Omega} = \sqrt{4\omega_f^2 - \Gamma^2}$. We note, that for the deep underdamped regime $\omega_f \gg \Gamma$, as verified in the main text, then

$$
\sigma_{xx}(t) = \sigma_i \frac{\chi - 1}{2\chi} \left[1 + \cos \left(2\omega_f t \right) \right] e^{-\Gamma t} + \frac{\sigma_i}{\chi}. \tag{S4}
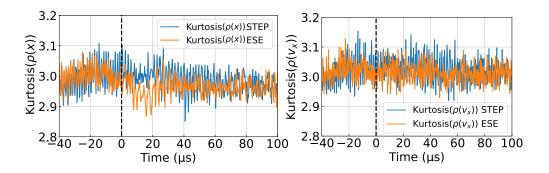$$

The oscillation frequency observed during the STEP protocols is then twice the natural final frequency of the trap ω_f.

Experimentally, we fit the experimental data computed for the position variance $\sigma_{xx} = \sigma_x^2$ using equation (S3), with Γ and ω_f as free parameters. The results are presented in figure S3. In the main text (Figure 2(b)), we plot the square-root counterpart, to depict the position standard deviation σ_x.

Supplementary Figure S3. Position variance σ_{xx} (black line) during a STEP protocol and associated fit. The fit allows us to determine the values of $\omega_{\text{relax}} = 2\omega_f$ and Γ. The timebase has been corrected to enforce $t_0 = 0$ µs.

VI. KURTOSIS FOR STEP AND ESE PROTOCOLS

Supplementary Figure S4. Kurtosis of $\rho(x)$ and $\rho(v_x)$ during STEP and ESE protocols

The kurtosis of the particle distribution along the position x axis $\rho(x)$ and velocity axis $\rho(v_x)$ during STEP and ESE protocols is shown in figure S4. The measured kurtosis remains very close from 3, demonstrating that, if existing, deviation from Gaussianity remains small.

VII. LINK BETWEEN THE ESE VARIABLES AND THE VELOCITY AND POSITION VARIANCE

The shortcut protocols used in the main text enforce a probability density for the system of the form

$$\rho(x,v,t) = N_0 \exp(-(\alpha(t)x^2 + \beta(t)v^2 + \delta(t)xv)) \tag{S5}$$

For such a distribution, one can compute the quantities σ_{xx}, σ_{vv} and σ_{vx}. We can thus determine the value of α, β and δ :

$$\alpha = \frac{\sigma_{vv}}{2(\sigma_{vv}\sigma_{xx} - \sigma_{xv}^2)}, \quad \beta = \frac{\sigma_{xx}}{2(\sigma_{vv}\sigma_{xx} - \sigma_{xv}^2)}$$

$$\delta = \frac{-\sigma_{xv}}{(\sigma_{vv}\sigma_{xx} - \sigma_{xv}^2)}$$

In the main text (Figure 2(d)), we thus reconstruct the PDF of the system during the ESE process, by computing the values of α, β and δ from the position variance σ_{xx}, the velocity variance σ_{vv} and the cross-correlated term σ_{xv}.

Conversely, if α, β and δ are known, one can compute the values of σ_x and σ_{v_x} as shown in figures 2b and c of the main text.

VIII.   DEFINITION OF THE ESE PROTOCOLS

A.   The "protocol A" solution

The ESE protocols used in the main text are the type defined as "*protocol A*" in reference [4]. The idea behind this work is to engineer the evolution of the distribution

$$\rho(x, v_x, t) = N(t) \exp(-(\alpha(t)x^2 + \beta(t)v_x^2 + \delta(t)xv_x)), \tag{S6}$$

via the control parameter k_{trap}. Injecting this Ansatz into the Fokker-Planck equation:

$$\frac{\partial \rho}{\partial t} + v_x \frac{\partial \rho}{\partial x} - \frac{k_{\text{trap}}}{m} x \frac{\partial \rho}{\partial v_x} = \frac{\Gamma}{m} \frac{\partial v_x \rho}{\partial v_x} + \frac{\Gamma k_B T}{m^2} \frac{\partial^2 \rho}{\partial v_x^2}, \tag{S7}$$

provides a set of non-linear equations linking the rescaled functions

$$\begin{cases} \tilde{\kappa} &= \dfrac{k_{\text{trap}}}{k_i} \\ \tilde{\alpha} &= \dfrac{2k_B T}{k_i}\alpha \\ \tilde{\beta} &= \dfrac{2k_B T}{k_i}\beta \\ \tilde{\delta} &= \dfrac{2k_B T}{k_i}\delta \end{cases}$$

expressed in rescaled time $s = t/t_f$.

Introducing the auxiliary quantity

$$\tilde{\Delta} = (\tilde{\alpha} - \frac{\tilde{\delta}^2}{\tilde{\beta}})\tilde{\beta}, \tag{S8}$$

allows rewriting the aforementioned functions in terms of $\tilde{\Delta}$. Thus, to define a protocol, all that is needed is to find a $\tilde{\Delta}$ which satisfies the boundary conditions on $\tilde{\alpha}$, $\tilde{\beta}$ and $\tilde{\delta}$, in particular $\tilde{\alpha}(1) = \tilde{\Delta}(1) = \chi$. In reference [4], to ensure continuity of the control parameter k_{trap}, the two first derivative of $\tilde{\Delta}$ are taken to be 0 in $s = 0$ and $s = 1$.

Finally, the control parameter $k_{\text{trap}} = k_i \cdot \tilde{\kappa}$ is then fully defined as:

$$\tilde{\kappa} = \frac{\dot{\tilde{\alpha}}}{2\omega_i \tilde{\delta}} + \frac{\Gamma}{\omega_i} \tilde{\delta} \,, \tag{S9}$$

Following Chupeau et al. [4], we look for a polynomial solution for $\tilde{\Delta}$. The lower order admissible polynomial is then:

$$\tilde{\Delta}(s) = 1 + (\chi - 1)(35s^4 - 84s^5 + 70s^6 - 20s^7) \,. \tag{S10}$$

All the ESE protocols shown in the main text are based on this approach.

B. Alternative ESE protocols

Nevertheless, we note that the choice of $\tilde{\Delta}(s)$ is arbitrary, and one could imagine using a different function, a higher order polynomial, or a different basis for the decomposition. For instance, one can use a sinusoidal basis. The lower admissible order then leads to

$$\tilde{\Delta}_{\text{sin}}(s) = \frac{1 + \chi}{2} + 9\frac{1 - \chi}{16} \cos(\pi s) - \frac{1 - \chi}{16} \cos(3\pi s) \,. \tag{S11}$$

Experimentally, using this protocol provides similar results to those obtained with the polynomial *Protocol A* described previously.

IX. HEAT AND WORK FOR THE USED PROTOCOLS

From the particle time traces, we can compute the cumulative heat

$$\langle Q(t) \rangle = - \int_0^t k(t') \langle x v_x \rangle \mathrm{d}t' - \left[\frac{1}{2} m \langle v_x^2 \rangle \right]_0^t = \langle Q_x(t) \rangle + \langle Q_v(t) \rangle \,, \qquad (S12)$$
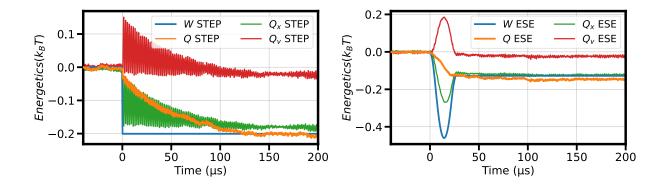
and the cumulative work

$$\langle W(t) \rangle = \int_0^t \frac{1}{2} \dot{k}(t') \langle x^2 \rangle \mathrm{d}t' \,, \qquad (S13)$$

exchanged between the system and the environment for the STEP and the shortcut protocol presented in figure 2 of the main text. The results are shown in figure S5.

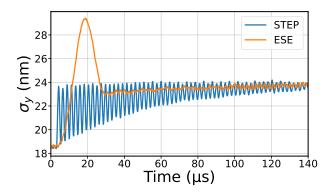In the case of a STEP protocol, the cumulative work is estimated from its theoretical value

$$\langle W(t) \rangle = \frac{\chi - 1}{2} k_B T \qquad (S14)$$

for any positive time.

Supplementary Figure S5. Heat and work for a STEP protocol (a) and the equivalent shortcut ESE protocol presented in the main text (b). The work for the STEP protocol is obtained from Eq. (S14).

X. RELAXATION ALONG THE y-AXIS

Supplementary Figure S6. Relaxation along the y-axis for the STEP (blue) and ESE (orange) protocols, the latter targeting acceleration equilibration along the x-axis to $t_f = 26$ µs, as shown in figure 3a in the main text. As for the z-axis, relaxation to equilibrium is observed in the target time for moderate speed-up (here 5-fold).

XI. STATE-TO-STATE PROTOCOLS ROBUSTNESS

To address the robustness of a transformation protocol defined for a reference system, we propose to characterize how close from equilibrium ends an arbitrary system submitted to this protocol.

To characterize this distance to equilibrium between the system distribution at the end of the protocol $p(x, v)$ and the equilibrium distribution $q(x, v)$, we use the Kullback–Leibler divergence $D(p||q)$. This estimator is defined as

$$D(p||q) = \iint \mathrm{d}x\mathrm{d}v \, p(x, v) \ln \left(\frac{p(x, v)}{q(x, v)} \right) , \tag{S15}$$

and can be seen as a statistical distance between the two distributions p and q.

In the present paper, we are interested in the efficiency of an ESE protocol defined for a system of natural frequency ω_{ref} applied to a system of frequency ω (the second axis in the main text). We thus determine the ESE protocol corresponding to a system of natural frequency ω_{ref} and damping Γ, and for a final time t_f. We then numerically compute the evolution of the distribution

$$\rho(x, v_x, t) = \frac{\sqrt{4\alpha(t)\beta(t) - \delta(t)^2}}{2\pi} e^{-\alpha(t)x^2 - \beta(t)v^2 - \delta(t)xv} \tag{S16}$$

of a system of frequency ω submitted to the protocol (same damping, same final time). This is done by numerical integration of the set of equations (14) in reference [4]. We thus compute the final value of the distribution $p(x,v) = \rho(x, v_x, t_f)$

By considering the equilibrium target distribution

$$q(x,v) = \rho_{\text{eq}}(x, v_x, t_f) = \frac{m\omega\chi}{\pi k_B T} \exp\left(-\chi\frac{m\Omega_i^2}{k_b T}x^2 - \frac{m}{k_b T}v^2\right), \tag{S17}$$
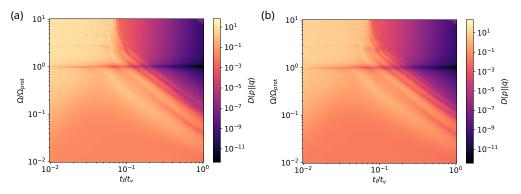
one can write the Kullback-Leibler divergence as:

$$D(p||q) = \frac{1}{2}\ln\left[\frac{4\alpha\beta - \delta^2}{4\alpha^{\text{eq}}\beta^{\text{eq}}}\right] - (\alpha - \alpha^{\text{eq}})\sigma_{xx}^f - (\beta - \beta^{\text{eq}})\sigma_{vv}^f - \delta\sigma_{xv}^f, \tag{S18}$$

where

$$\begin{cases} \sigma_{xx} = \langle x^2 \rangle = \dfrac{2\beta}{4\alpha\beta - \delta^2} \\ \sigma_{vv} = \langle v^2 \rangle = \dfrac{2\alpha}{4\alpha\beta - \delta^2} \\ \sigma_{xv} = \langle xv \rangle = \dfrac{-\delta}{4\alpha\beta - \delta^2} \end{cases}$$

The Kullback-Leibler divergence for the ESE protocols as a function of the final time t_f and the frequency difference $\omega/\omega_{\text{ref}}$ is shown in figure S7-(a).

Supplementary Figure S7. Kullback-Leibler divergence for the ESE protocols as a function of the final time t_f and the system frequency ω. (a) Protocol used in the main text. (b) Alternative sinusoidal protocol defined by equation S11.

A couple of interesting features are observed. First, the protocols are more robust for moderate acceleration, as discussed for experimental data in the main text. Then, the evolution of the Kullback-Leibler divergence is non-monotonic, and we observe a coupling between frequency and final time impacting protocol robustness. As a consequence, for a given system frequency ω, tuning the final time to reach a state closer to equilibrium could be interesting.

To discuss the universality of these features, we apply the same procedure for the protocols defined in the previous part, which use a sinusoidal decomposition for the Δ function (see equation S11). The results are presented in figure S7-(b), demonstrating the same properties, with a worse protocols efficiency for decreasing final time and the non-monotonic behaviour of the Kullback-Liebler divergence.

Finally, we demonstrate that Kullback-Leibler divergence could be a strategy to characterize the robustness of state-to-state protocols. If the two proposed protocols share the same limitation to moderate speed-up, our strategy could be used to discuss other protocols, both for swift equilibration and optimization protocols [5].

[1] J. Gieseler, B. Deutsch, R. Quidant, and L. Novotny, Phys. Rev. Lett. **109**, 103603 (2012).

[2] I. A. Martínez, A. Petrosyan, D. Guéry-Odelin, E. Trizac, and S. Ciliberto, Nat. Phys. **12**, 843 (2016).

[3] C. Zerbe, P. Jung, and P. Hänggi, Phys. Rev. E **49**, 3626 (1994).

[4] M. Chupeau, S. Ciliberto, D. Guéry-Odelin, and E. Trizac, New Journal of Physics **20**, 075003 (2018).

[5] P. Muratore-Ginanneschi and K. Schwieger, Phys. Rev. E **90**, 060102 (2014).